Advanced imaging system with multiple optical sensing modes

Kyle McCormick*[a], Jaclyn M. Nascimento[a], Leif Hendricks[a]
[a]Surface Optics Corporation, 11555 Rancho Bernardo Rd., San Diego, CA, USA 92127-1441

ABSTRACT

The Spectral-Polarimetric Hypersensor (SPH) is a new compact, solid state, video rate imaging system with no moving parts capable of capturing up to 16 bands of both spectral and polarimetric content simultaneously. For these imagers, which are an adaptation of a plenoptic system, all elements for a given super pixel sample the same point in the scene, thus providing the ability to accurately measure point sources. Various scenes are imaged using two systems that span the VNIR (0.4 – 0.95nm) and SWIR (0.9-1.7μm) wavebands. For each imager, twelve spectral components and four polarization states are captured simultaneously. The VNIR system captures full data cubes of 512x512 (spatial pixels) x 12 (spectral bands) x 4 (polarization states) at frame rates up to 30 Hz while the SWIR system captures full data cubes of 320x256 (spatial pixels) x 12 (spectral) x 4 (polarization states) at frame rates up to 30 Hz. From the acquired images, we compute the Stokes vector components, calculate DoLP, polarization angle, and obtain a spectral signature of objects in the scene. This data is then used to carry out target identification and clutter suppression in real-time, i.e. video frame rates.

Keywords: real-time, multi-modal, spectral imaging, polarimetric imaging, plenoptic, VNIR, SWIR, hypersensor

1. INTRODUCTION

Conventional imaging systems are typically based on a single or combination of broadband sensors operating across all wavebands (from the Visible to Near-Infrared (VNIR) to the longwave infrared (LWIR)). The sensors record the reflected and/or emitted radiation coming from a target of interest to detect and discriminate it from the background or other target like objects. For defense applications, they are compact, rugged, and lightweight and generally image at video frame rates or higher to support targeting and/or guidance. VNIR imagers can be monochromatic or color and may include a near-infrared channel to discriminate vegetation. SWIR imagers sense radiance differences that are the result of changes in reflected energy just outside the visible region (0.9 – 1.7 microns) and can be used to defeat conventional visible camouflage.

In addition to these broadband systems, multispectral/hyperspectral imaging systems collect multiple bands simultaneously on a single sensor for a given sensor spectral response. These imaging systems can collect 'color' information at a much finer spectral resolution than a simple 3-color RGB camera. In the VNIR, they can be used to detect subtle color differences not visible to the human eye and for the SWIR they can provide precise identification of chemical compounds.

Polarimetric imaging is another technique which records the polarization properties of an object which contains unique and important information not found in the other systems. For example, the degree of polarization can yield information about the roughness and material of the target surface, while polarization orientation can indicate direction of the surface facet normal. Tyo, *et al.*[1] describes some of the advantages and disadvantages of polarization imaging from the VNIR through the LWIR. Figure 1 shows a standard RGB image from a VNIR imager alongside Degree of Linear Polarization (DoLP) and Angle of Linear Polarization (AoLP) images taken with Surface Optics Corporation's (SOC) SWIR Hypersensor modified to capture polarimetric data. The images show a truck and miscellaneous targets, e.g. plexiglass and camouflage fabric, in the back parking lot at SOC. The information content in the image is exemplified by the uniformity in the hood of the vehicle, which has a high value in the DoLP indicating a large degree of polarization, i.e. human-made, and in the AoLP image which indicates that the hood is a large facet oriented vertically. Also, notice the plexiglass panel which is not so readily visible in the RGB image shows up clearly as a dark rectangle in the DoLP and as uniformly bright in the AoLP image.

Figure 1. SWIR Image of Truck – Reference image in RGB (left), SWIR DoLP (center) and SWIR AoLP (right).

Recently, the combination of spectral and polarimetric imaging has shown to provide an advantage over conventional imaging, providing a more complete representation of objects in a scene. A review of applications for multiband polarization imaging can be found in Zhao, *et al*[2]. The applications include medical diagnosis, image dehazing, and surveillance and reconnaissance. For the latter application, the effective use of signature control technologies, whether active or passive, can mitigate the effectiveness of a given conventional spectral or polarimetric sensor and can make targets more difficult to detect. Additionally, differentiation among target types that have been detected, e.g., tracked versus wheeled vehicles, is not a capability readily available and system performance is degraded in the presence of background clutter. Typically, to overcome the effects of various signature control technologies, a suite of sensors, known as multi-modal imaging systems, have been developed that include several spectral and/or polarization sensors. These systems, however, are generally large, relatively cumbersome, and require significant amounts of processing power for image registration and alignment.

Surface Optics Corporation (SOC) presents its plenoptic imaging system as a solution to capture multiple optical sensing modes simultaneously in real time. The Spectral-Polarimetric Hypersensor (SPH) is a highly compact, solid state, video rate imaging system with no moving parts capable of capturing four polarization components and up to twelve spectral components simultaneously within each resolution element (i.e. pixel) of the imagery. The polarization, as well as the spectral, information, is valid for measuring point sources within the scene since all elements for a pixel sample the same point in the scene avoiding potential registration issues. Measurements are available at the full frame rate of the camera.

The polarization and spectral filter elements of the system are large-scale by design, which greatly improves the element quality, reduces fabrication cost and easily accommodates infrared filters. By placing the filters/polarizers in a convenient, replaceable tray at the optical pupil of the system, the Hypersensor is not only compact, but it also offers spectral 'flexibility' via a simple filter/polarizer tray substitution which can be tailored to various targets or applications.

This paper presents two of SOC's imaging systems that were adapted for multi-modal sensing. The VNIR imaging system captures full data cubes of 512x512 (spatial pixels) x 12 (spectral bands) x 4 (polarization states) simultaneously at frame rates up to 30 Hz. The SWIR imager, although capable of also capturing 12 spectral and 4 polarization states simultaneously, had two filter tray sets (one housing 16 spectral bands, the other housing 4 polarization filters). Nonetheless, the system's processed data cubes are 320x256 (spatial pixels) x 12 (spectral) x 4 (polarization states). The majority of the effort focused on developing the calibration methodology, calibrating the units themselves, and identifying the proper handling techniques and tooling required. Various scenes were then imaged and analyzed. The Stokes vector components, Degree of Linear Polarization (DoLP), Angle of Linear Polarization (AoLP), and a spectral signature of objects in the scene were all measured.

2. METHOD

2.1 Hardware

SOC has developed and demonstrated multiple 9-band and 16-band full-motion video hypersensor spectral imagers, operating in bands from 270 nm to 5.0 μm. The imaging approach embodied by these imagers, and outlined in Figure 2,

records a complete multimodal image, be it spectral or polarimetric, with each exposure of the focal plane. These spectral image cubes are generated at the full frame rate of the camera, which is 30 Hz or greater in our current camera systems. This approach and variants of it are applicable to all wavebands, including VNIR, SWIR, and MWIR.

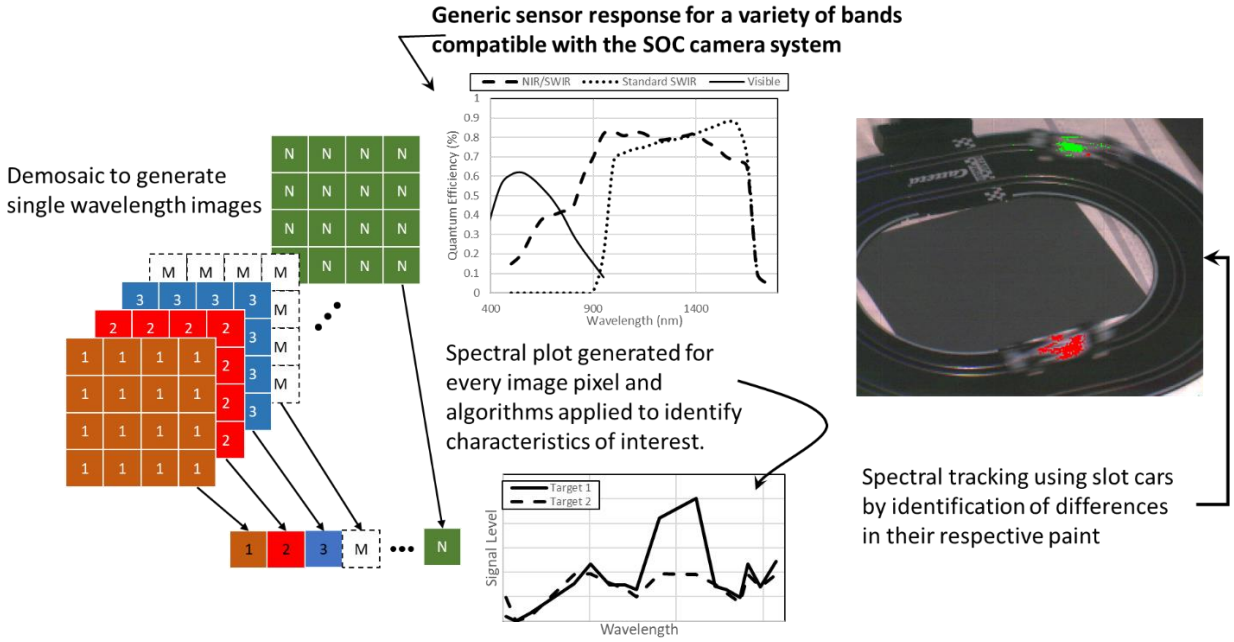

Figure 2. Surface Optics spectral imaging technology separates the spectral components of the imaged scene to allow for object tracking and detection.

Table 1 below presents some of SOC's developed imagers and highlights the real-time processing capabilities. In house, SOC has several demonstration units available. The VNIR (400nm – 950nm) imager is shown in Figure 3a. The SWIR (0.9µm – 1.7µm) imager is shown in Figure 3b.

Table 1. Hypersensor instruments developed by SOC.

	FPA Technology	Pixel Pitch	Full Cube Resolution
UV	CCD with Lumogen Coating	7.4µm	512 x 512 x 16
VNIR	CCD	7.4µm	512 x 512 x 16
SWIR	InGaAs	12µm	320 x 256 x 16
MWIR	InSb or nBn	12µm	320 x 256 x 16
Processing	Integrated modified SOC MIDIS real-time hyperspectral image processor, capable of sustained 500 Mpixel-per-second throughput		

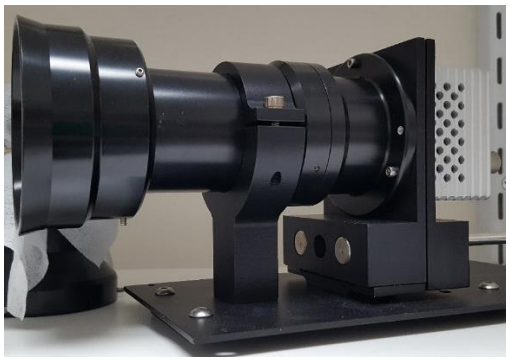

Figure 3a. SOC's VNIR Hypersensor Imager – Data cube is 512 x 512 spatial pixels x 16 filters. Filters can be any combination of spectral and polarimetric. Sensor operates from 400nm – 950nm.

Figure 3b. SOC's SWIR Hypersensor Imager – Data cube is 320 x 256 spatial pixels x 16 filters. Filters can be any combination of spectral and polarimetric. Sensor operates from 0.9μm – 1.7μm.

The filter trays (not visible in Figure 3) reside at the front of the lens. This configuration makes it very convenient to replace the filter tray, providing filter 'flexibility' through tray substitution. As such, only a new filter tray for each system shown was necessary. For the VNIR system, the tray was populated with readily available COTS spectral filters and four polarizers (Figure 4a). The four polarization filters' transmission axes were 0º, 45º, 90º, and 135º. Figure 4b shows the transmission curves of the spectral filters as populated in the tray (actual transmission for a given tray is necessary for calibration). The SWIR polarizer filters, also with transmission axes of 0º, 45º, 90º, and 135º, were populated in a tray without spectral filters (spectral filter tray was separate; not shown). Notice the reference mark for the VNIR tray (Figure 4a) in the upper left and the dowel pin configuration, which ensure the filter tray is mounted in the same orientation every time.

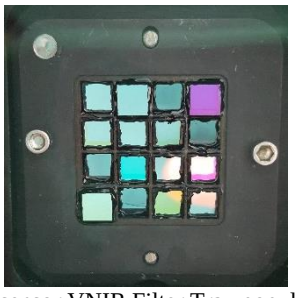

Figure 4a. Spectral-Polarimetric Hypersensor VNIR Filter Tray populated with both spectral and polarizer filters.

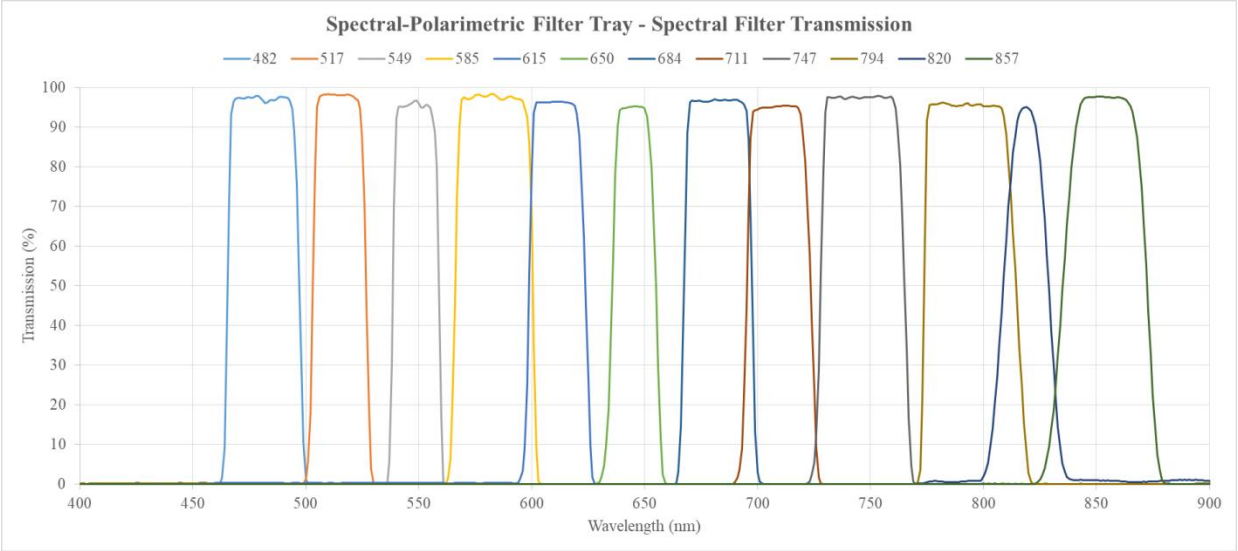

Figure 4b. Spectral-Polarimetric Hypersensor VNIR Filter Tray – spectral filter transmission curves.

2.2 Calibration

To extract meaningful data from the polarization images, the system must be calibrated. The proven process for calibrating SOC's Spectral Hypersensor systems is still valid for properly extracting the image and accounting for various effects even when using the polarizer filters. However, an additional polarization calibration process is required to account for any uncertainty or error in the polarization filters' relative transmission axes. SOC followed the technique laid out by Farlow *et al*[3]. In this process, SOC utilized Mueller matrices and created a calibrated analyzer matrix for the system using the following equation: $I = P * S$. It is a fairly straightforward equation, containing the intensity measured at the detector (I), the Stokes vector (S) and the analyzer matrix (P). By controlling S in the calibration steps (i.e. using a known input polarization), the resulting intensity values can be measured and then subsequently one can calculate the analyzer matrix. The analyzer matrix can then be applied to the received intensity from any given scene, and the incident Stokes vector can be calculated. In order to do this, the equation above is simply adjusted:

$$P = I * S^{-1}$$

to calculate the analyzer matrix from the calibrated input. Then subsequently:

$$S = P^{-1} * I$$

to measure the Stokes vector of the scene.

This simple method of calibration is particularly valuable due to the differences that are expected from slight rotations from theoretical. With a system calibrated to known inputs, inverting the analyzer matrix now provides straightforward matrix multiplication to retrieve the Stokes parameters from any point in the image. In the process of obtaining the calibration table, data was verified against theoretical to ensure it was being implemented accurately as well as to check the alignment accuracy of the polarizers. Combining and organizing the matrices, it was shown that the expected (theoretical) and actual (measured) data were in good agreement. Figure 5 presents the comparison of the expected matrix from the theoretical system and the calibrated output from the actual system. Deviations from theoretical are present, indicating the polarizer filter elements and the calibration polarizer are not perfectly aligned. However, the two matrices are in relatively good agreement.

$$P_{expected} = \begin{bmatrix} 0.5 & 0.5 & 0 & 0 \\ 0.5 & -0.5 & 0 & 0 \\ 0.5 & 0 & 0.5 & 0 \\ 0.5 & 0 & -0.5 & 0 \end{bmatrix} \quad P_{actual} = \begin{bmatrix} 0.4677 & 0.3587 & -0.0159 & 0 \\ 0.4154 & -0.305 & 0.0207 & 0 \\ 0.548 & -0.026 & 0.4519 & 0 \\ 0.4856 & 0.0295 & -0.3754 & 0 \end{bmatrix}$$

Figure 5. Measured vs. Expected Analyzer Matrix – The deviations from the expected 0.5 values show that the polarizers are not perfectly aligned, rather some amount off the theoretical. The measured matrix follows the same trend while still being in relatively good agreement.

In the implementation of the conversion matrix, a single calibration matrix for the full array would be the simplest, most straightforward method. Unfortunately, our system shows variation across the sensor which introduces inaccuracies when calculating the polarization. Therefore, a single calibration matrix is insufficient and pixel specific analyzer arrays must be used. An example of the variation across the image sensor can be seen in Figure 6.

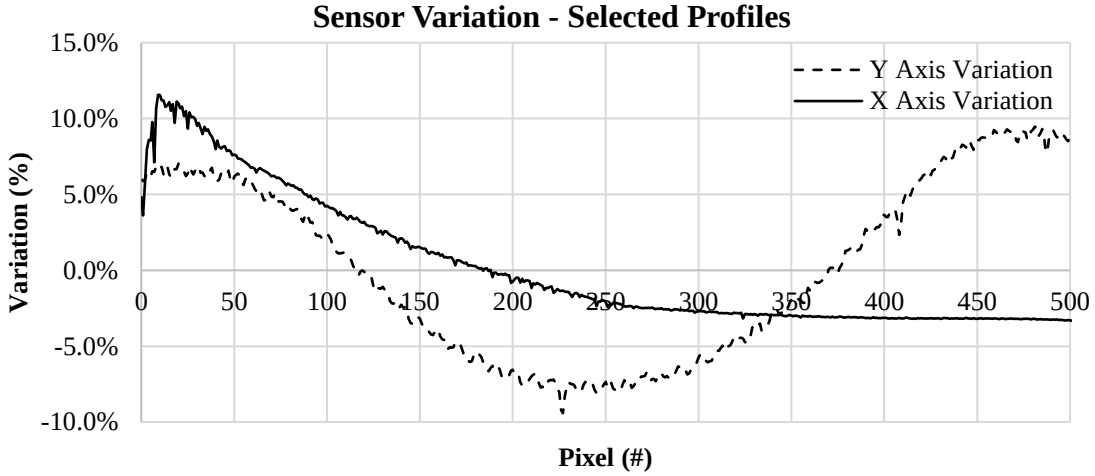

Figure 6. A set of selected sensor cross sections showing the sensors signal variation across the vertical and horizontal axes. This variation makes a single calibration function impossible and also shows areas for improvement with our latest design.

Having completed the calibration, it is now possible to accurately capture the well-defined functions of Degree of Linear Polarization (DoLP) and Angle of Linear Polarization (AoLP) (equations below) on a per-pixel basis using the instrument.

$$DoLP = \frac{\sqrt{S_1^2 + S_2^2}}{S_0}$$

$$AoLP = \frac{1}{2}\tan^{-1}\left(\frac{S_2}{S_1}\right)$$

3. RESULTS

3.1 VNIR imagery

3.1.1 Simultaneous acquisition of spectral and polarimetric bands

Spectral and polarimetric data was simultaneously captured using a variant of SOC's VNIR Hypersensor. Figure 7 shows an acquired image in its raw format (that which the FPA acquires) along with a mosaic of the sub-aperture images, successfully demonstrating how both spectral and polarimetric images can be acquired simultaneously.

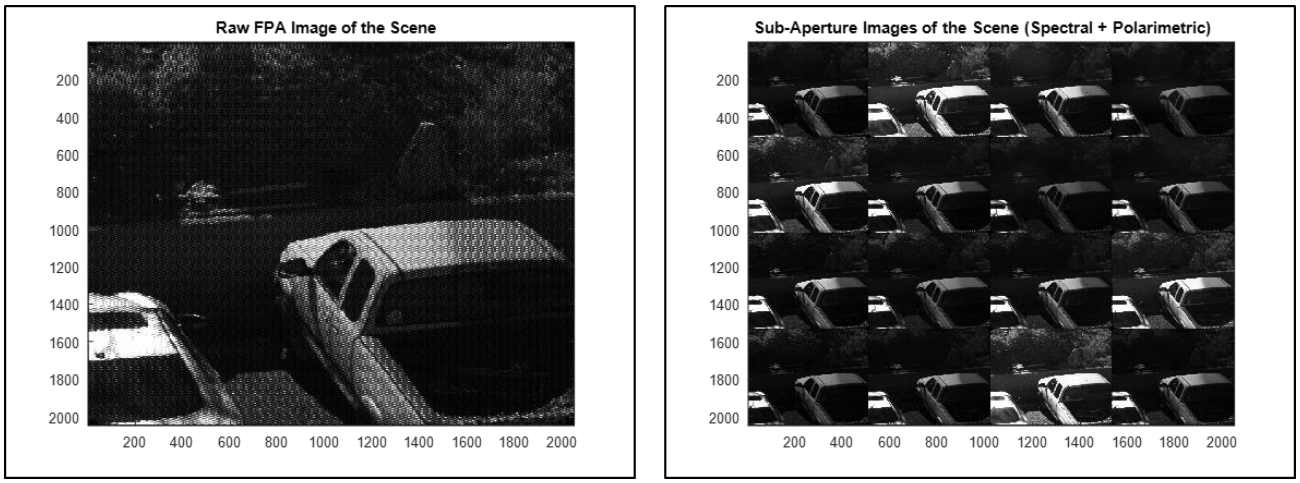

Figure 7. Simultaneous Acquisition of Spectral and Polarimetric Bands – The raw FPA image (left) of the scene is broken into the sub-aperture images (right).

3.1.2 Narrow band spectral vs. broad band polarimetric imaging and energy balancing

The broadband polarizers admit more light and require much shorter integration times than that of the narrow band spectral filters. During data collection, it became apparent that in order to maximize the signal in the spectral bands, longer integration times were required. However, this resulted in saturating the polarization bands. Figure 8 shows the sub-aperture image at two integration times. At the low integration time (IT), the signal in the polarimetric images is optimized, having a maximum signal just below saturation of 4096 counts. Unfortunately, this causes more of the light starved bands, such as center wavelengths 820nm or 857nm, to have very poor signal levels and much of the data is lost in the noise. At high IT, the spectral bands show cleaner signals; however, the polarizer images are saturated. Figure 9a, b, and c show the histograms of three representative bands (polarizer TA = 45º, CWL = 549nm and CWL = 820nm respectively) at both the low and high ITs. Again, the narrow band spectral filters require longer ITs to fill the histogram, but doing so would cause the polarizers to become saturated and thus useless. Note that the CWL = 820nm band could benefit from an even greater IT with respect to that of CWL = 549nm. This is because the FPA is less sensitive to these longer wavelengths, and the quantum efficiency drops after the green peak.

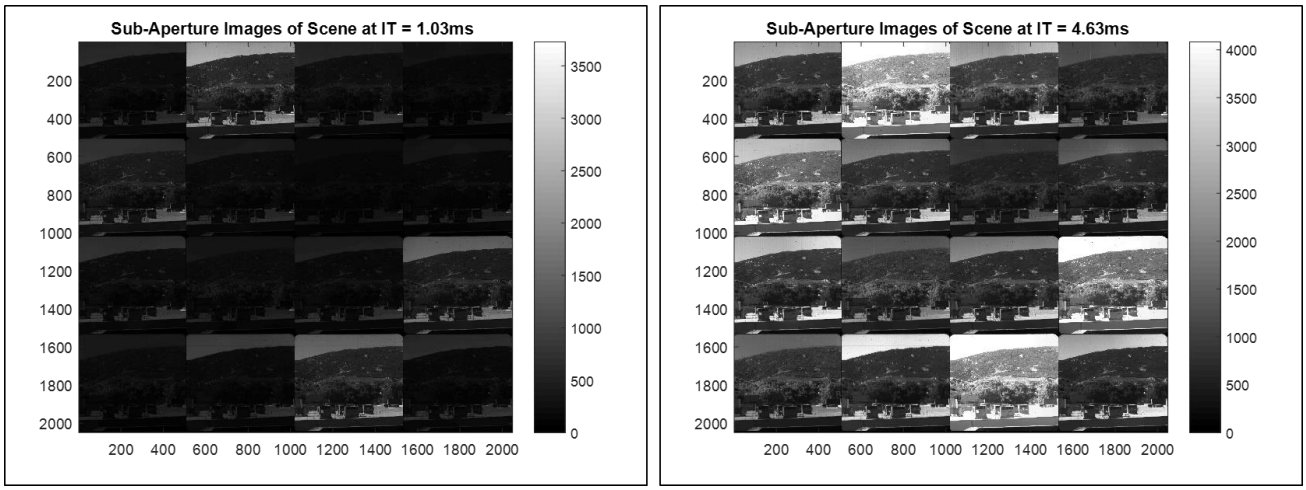

Figure 8. Sub-Aperture Images at Low and High Integration Times – For low IT, left, signal is optimized at the cost of the narrower, light starved spectral bands. For high IT, right, data in the spectral bands comes out of the noise floor, but the broadband polarizers are saturated.

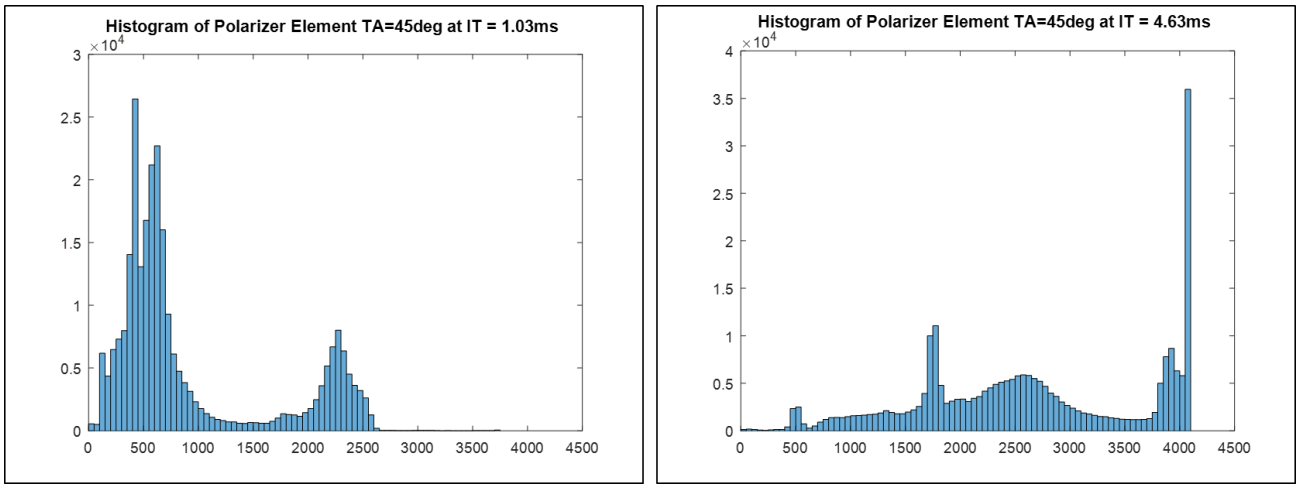

Figure 9a. Histograms of Polarizer (TA = 45º) Image – Low IT (left) is sufficient for the polarizer image to capture the scene data. High IT (right) pushes the band into undesirable saturation.

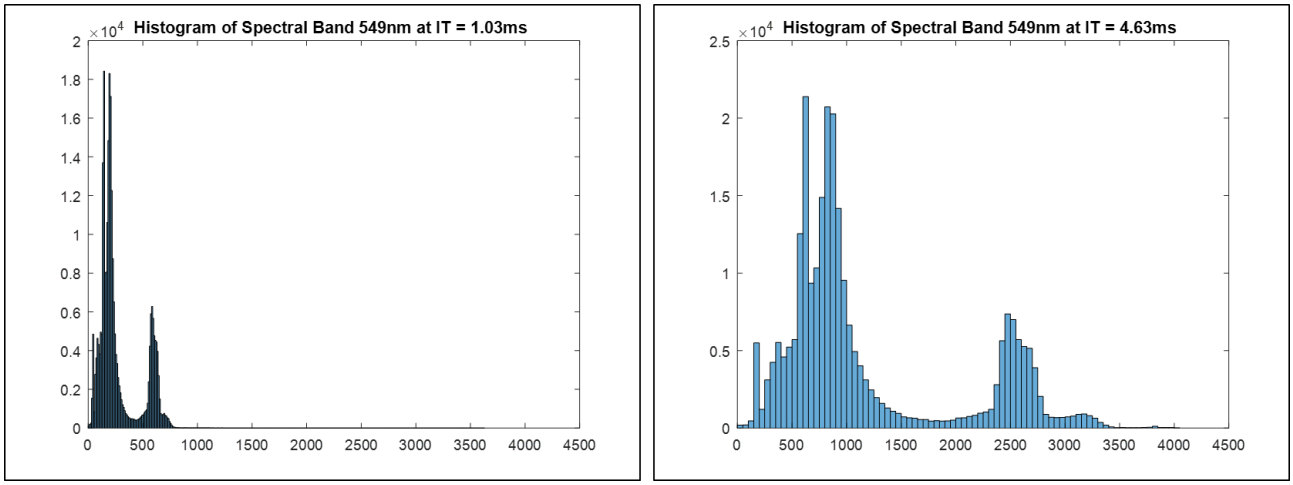

Figure 9b. Histograms of Spectral Band (CWL = 549nm) Image – Low IT (left) is insufficient for the narrow spectral band image to capture the scene data (information is near the noise floor). High IT (right) provides the needed exposure to capture scene data out of the noise.

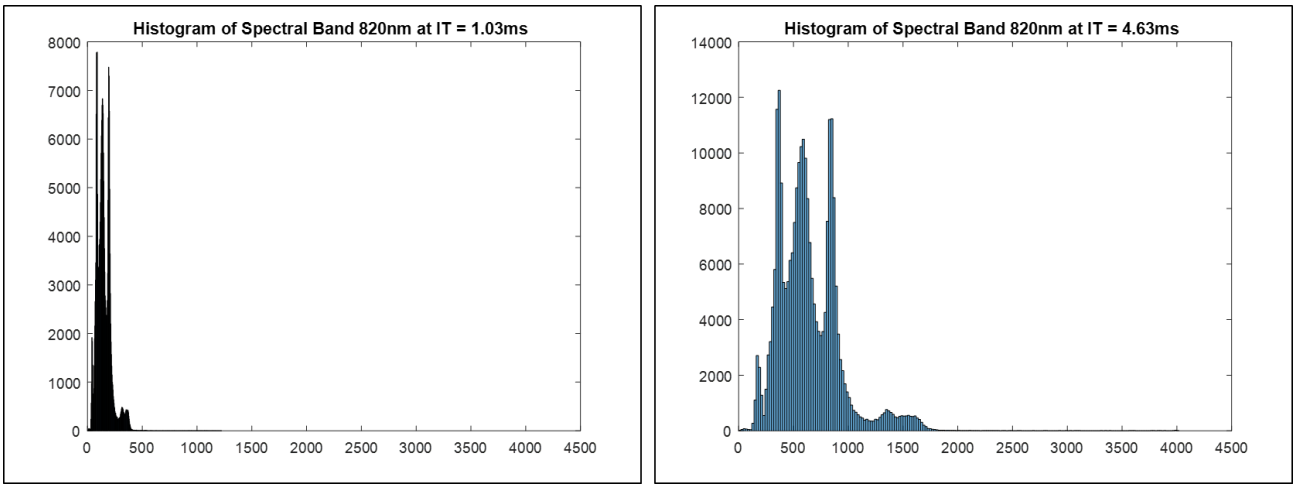

Figure 9c. Histograms of Spectral Band (CWL = 820nm) Image – Low IT (left) is insufficient for the narrow spectral band image to capture the scene data (information is near the noise floor). High IT (right) provides the needed exposure to capture scene data out of the noise.

There are solutions to equalize the energy disparity between the spectral and polarimetric bands. First, a super framing approach could be utilized. Alternating frames would be captured at low and high ITs. Extreme caution would be required here, as the saturated polarimetric pixel is physically adjacent to the spectral pixel and could degrade the integrity of the high IT spectral image. Another approach would be to place a mask at the filter plane to stop down the polarizer bands and allow the FPA to be operated at a single IT. Again, caution is required as the smaller the aperture, the higher the diffraction, causing additional bleed from the polarization pixel into the neighboring spectral pixels. A third solution would be to incorporate neutral density (ND) filters along with the polarizers in the filter tray itself. This presents itself as a good candidate, as it does not amplify the effects of diffraction nor does it require special software processing to handle the super framing. This remains to be investigated further.

3.2 SWIR imagery

3.2.1 Digital Focus/Refocusing Issues and Solution

The SWIR Hypersensor was retrofitted with four polarization filters. The polarization images were calibrated and used to calculate the DoLP of the scene. Figure 10 shows a SWIR polarimetric sub-aperture image as reference (left) and the calculated DoLP greater than 0.4 of the scene (right). The mountains in the distant background show a false high DoLP along the edge. This is due to the fact that the imager is focused on the cars in the foreground, making the mountains out of focus. When the four polarimetric images are used to calculate DoLP, it is obvious that out of focus objects can be falsely identified. Similar results have been encountered on previous programs that use spectral signatures to identify targets. Fortunately, given the nature of SOC's imagers, digital refocusing can correct for these false identifications.

Since SOC's plenoptic imagers measure the light field the object of interest in the scene will be focused onto the FPA, and objects nearer or farther will be out of focus. The out of focus light field in the plenoptic imager is simply a shifted version of the focused light field. By shifting the sub-aperture images, the images can be digitally refocused after acquisition. This can be done during post processing off-line, or in real-time using the high speed processor. Several papers on this topic are available (Georgiev and Lumsdaine[4], Ng, *et al.*[5], Adelson and Wang[6]).

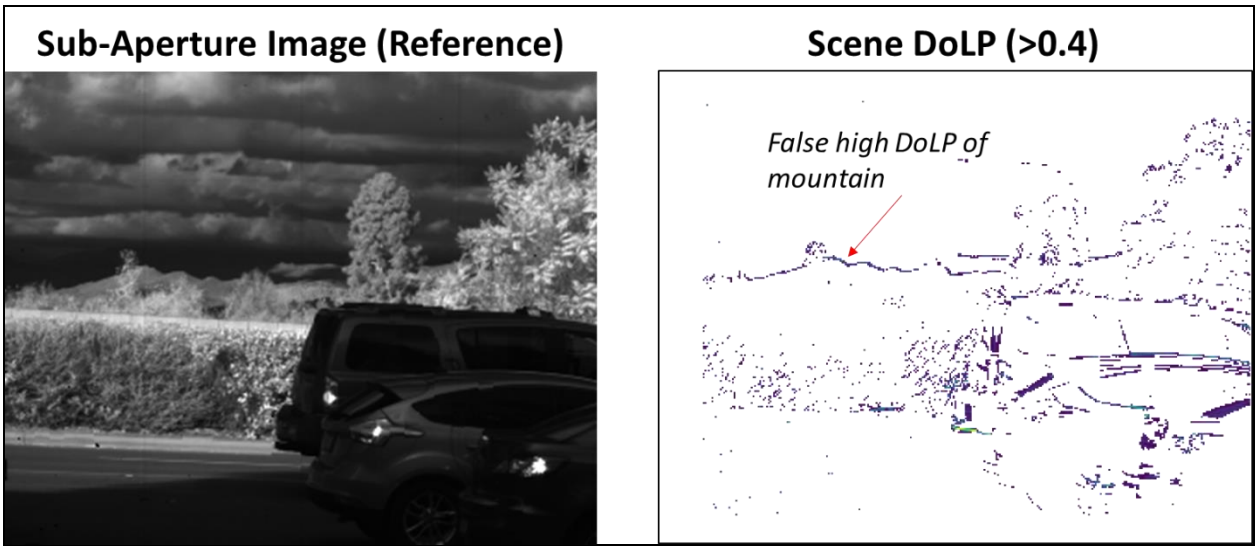

Figure 10. SWIR Polarimetric Image – High False DoLP: Out of focus mountains in background cause a false identification of DoLP. Reference image on left is one polarimetric sub-aperture image. Calculated DoLP (values >0.4) image on right.

SOC's plenoptic imagers rely on spectral purity for good target identification with low probability of false alarms. Even subtle shifts in focus can lead to noise on the spectral signature. SOC investigated implementing digital refocusing. Given a calibrated image, SOC implemented a solution to optimally refocus the entire image off-line. This algorithm was converted into C++ and added to the CUDA-based GUI for near real-time processing. Figure 11 below demonstrates the refocusing capabilities on SOC's VNIR imager. Three spectral wavebands were used to create the composite RGB image shown in the top row; top left is RGB image before refocusing and top right is the same after refocusing (centered on the human and panel in the center of the image). The bottom row of Figure 11 shows the summation of all 16 spectral wavebands both before and after refocusing (left and right respectively) of the same image. This provided proof of concept for SOC's plenoptic imagers. Further investigation and improvements are needed to correct for some distortion still evident in the refocused image. Additionally, the algorithm needs to be optimized for real-time processing. Completing this effort shall provide significant improvement for not only the spectral signatures of targets but also the DoLP and AoLP of the scene.

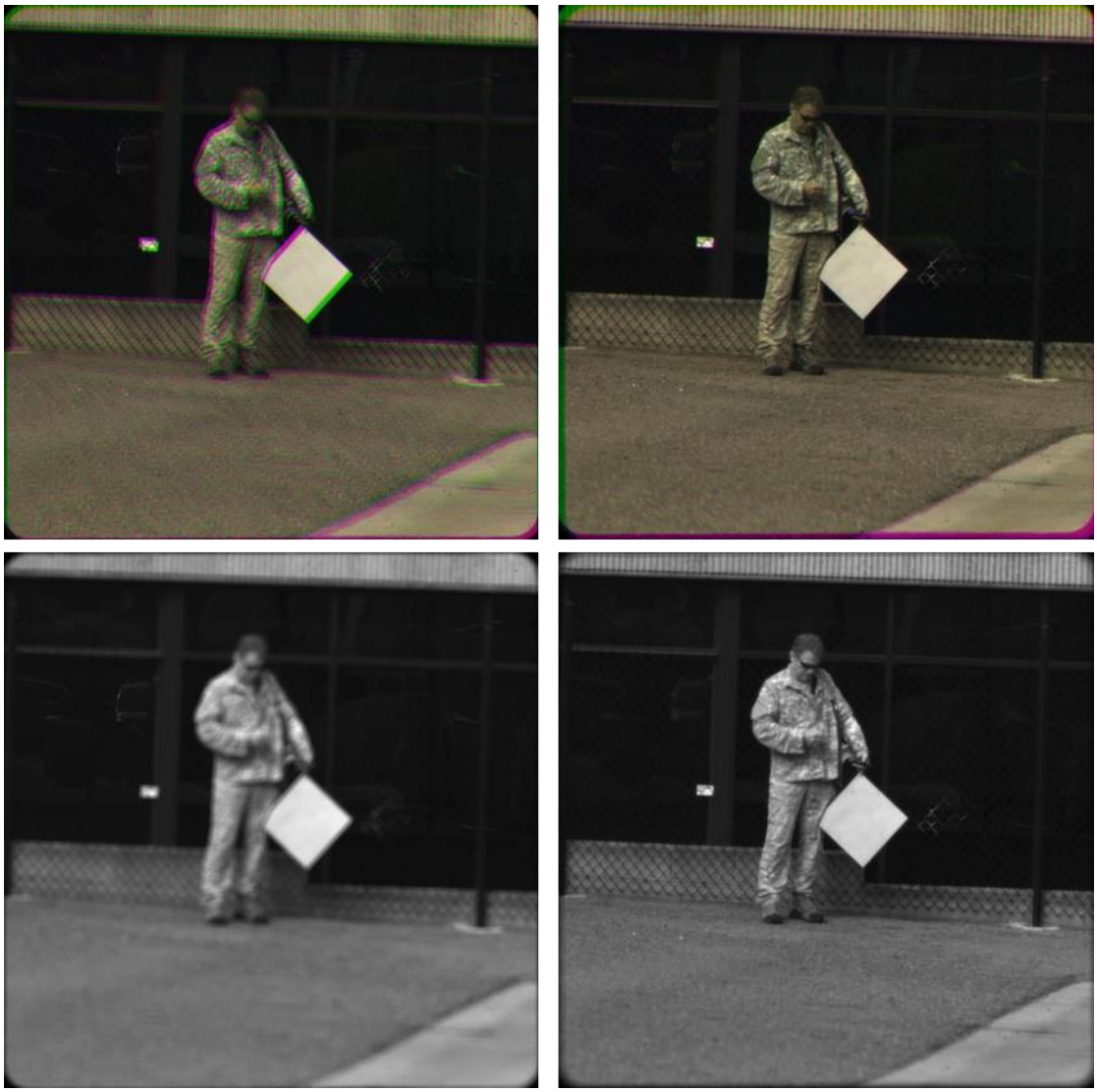

Figure 11. Digital Refocusing – Spectral VNIR imager used to show the ability of the post-processing refocusing algorithm to provide enhanced spectral and polarimetric signal purity. Top row: An RGB composite image both before (left) and after (right) refocusing. Bottom row: A composite of all 16 spectral waveband images both before (left) and after (right) refocusing.

3.2.2 SWIR DoLP and AoLP Images

Images were acquired of tops of trucks as they are well polarized surfaces. Figure 12 shows SWIR polarization data of the same scene as in Figure 1 with the plexiglass panel sitting in the shrubs along with other man-made items. As before, the plexiglass is readily discernable due to its low DoLP and uniform AoLP. A diagonal line in both images across the top of the roof of the truck coincides with a change in paint color from CARC tan (on the left) to CARC green (on the right) which could be indicative of changes in the formulations of the paint.

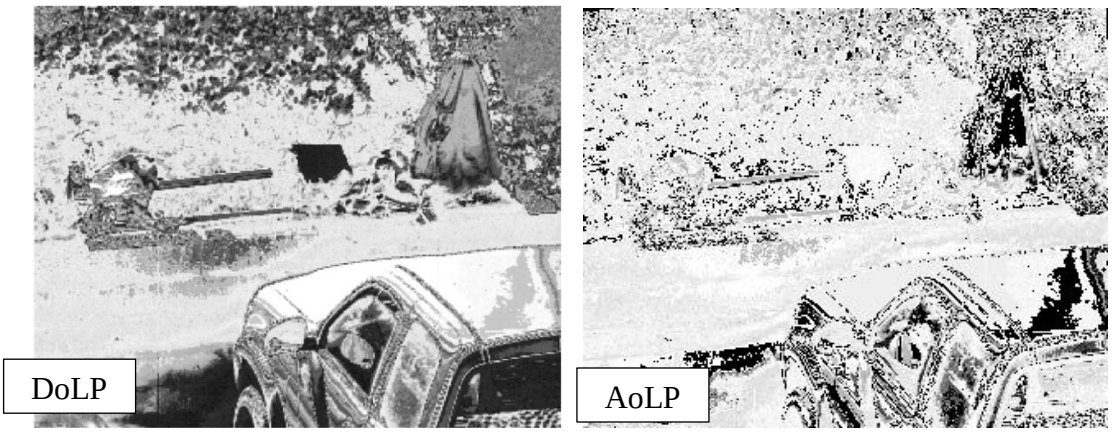

Figure 12. SWIR Image of truck and miscellaneous targets laid in the shrubs in the SOC parking lot. Note the uniform white across the hood of the vehicle. The diagonal line across the roof is indicative of the change in paints on SOC's specially painted vehicle.

Another validation point for the system was collected by looking at the sky (Figure 13), a source of highly polarized light due to scattering in the atmosphere. From the DoLP plot and the histogram showing the DoLP breakdown, it is confirmed that this indeed is the case. This confirms that the system is creating values consistent with what is expected as well as showing new avenues not anticipated.

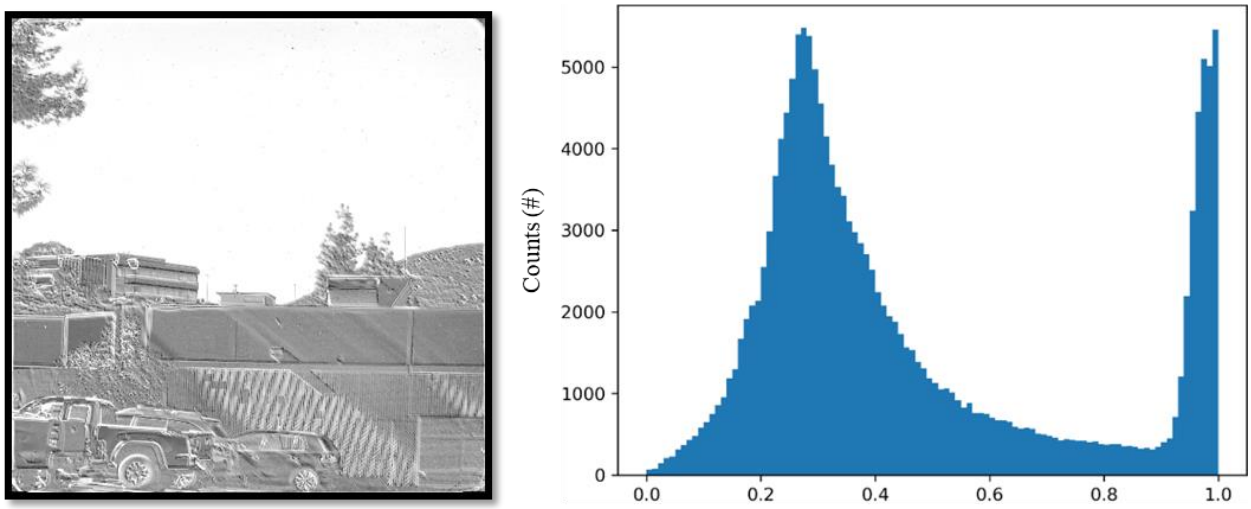

Figure 13. SWIR DoLP image (left) and the accompanying histogram (right) showing the polarized sky through the large spike in the polarization plot.

4. CONCLUSION

Using multiple optical sensing modes provides several advantages in various imaging applications, including target identification. SOC's imaging systems offer a unique method for capturing both spectral and polarimetric data simultaneously. In this paper, SOC has successfully demonstrated that these imagers can be adapted to capture these two optical sensing modes. The calibration methodology is presented. Additionally, limitations and potential solutions were identified; namely balancing the narrow band spectral filters and broad band polarizing filters, improvement in polarizer filter transmission and handling, and false DoLP of out of focus objects.

ACKNOWLEDGMENTS

This work was supported in part by the United States Air Force under Contract Number FA8651-17-P-0106 under the SBIR program and by SOC internal research and development funding. Any opinion, findings, and conclusions or recommendations expressed in this material are those of the author(s) and do not necessarily reflect the views of the USAF or the SBIR program.

REFERENCES

[1] Tyo, J.S., Goldstein, D.L., Chenault, D.B., Shaw, J.A., "Review of passive imaging polarimetry for remote sensing applications," Applied Optics 45(22), 5453-5469 (2006).
[2] Zhao, Y., Peng, Q., Yi, C. and Kong, S. G., "Multiband Polarization Imaging," J. Sensors 2016, 5985673 (2015).
[3] Farlow, C.A., Chenault, D. B., Pezzaniti, J. L., Spradley, K.D. , Gulley, M.G., "Imaging polarimeter development and applications," Proc. SPIE 4481, Polarization Analysis and Measurement IV, (2002); doi: 10.1117/12.452880; http://dx.doi.org/10.1117/12.452880.
[4] Georgiev, T., Lumsdaine, A., "Focused plenoptic camera and rendering," J. of Electronic Imaging 19(2), 021106 (2010).
[5] Ng, R., Levoy, M., Bredif, M., Duval, G., Horowitz, M., Hanrahan, P., "Light Field Photophraphy with a Hand-held Plenoptic Camera," Stanford Computer Science Technical Report CSTR (2005).
[6] Adelson, E. H., Wang, J. Y. A., "Single Lens Stereo with a Plenoptic Camera," IEEE Transactions on Pattern Analysis and Machine Intelligence 14(2), 99-106 (1992).